NASA
Technical Memorandum 88890

USAAVSCOM
Technical Report 86-C-38

Generation of a Composite Grid for Turbine Flows and Consideration of a Numerical Scheme

Y. Choo
Lewis Research Center
Cleveland, Ohio

and

S. Yoon
Sverdrup Technology, Inc.
Lewis Research Center
Cleveland, Ohio

and

C. Reno
Propulsion Directorate
U.S. Army Aviation Research and Technology Activity—AVSCOM
Lewis Research Center
Cleveland, Ohio

November 1986

NASA

GENERATION OF A COMPOSITE GRID FOR TURBINE FLOWS AND CONSIDERATION OF A NUMERICAL SCHEME

Y. Choo
National Aeronautics and Space Administration
Lewis Research Center
Cleveland, Ohio 44135

S. Yoon
Sverdrup Technology, Inc.
Lewis Research Center
Cleveland, Ohio 44135

and

C. Reno*
Propulsion Directorate
U.S. Army Aviation Research and Technology Activity - AVSCOM
Lewis Research Center
Cleveland, Ohio 44135

SUMMARY

A composite grid was generated for flows in turbines. It consisted of the C-grid (or O-grid) in the immediate vicinity of the blade and the H-grid in the middle of the blade passage between the C-grids and in the upstream region. This new composite grid provides better smoothness, resolution, and orthogonality than any single grid for a typical turbine blade with a large camber and rounded leading and trailing edges. The C-H (or O-H) composite grid has an unusual grid point that is connected to more than four neighboring nodes in two dimensions (more than six neighboring nodes in three dimensions). A finite-volume lower-upper (LU) implicit scheme to be used on this grid poses no problem and requires no special treatment because each interior cell of this composite grid has only four neighboring cells in two dimensions (six cells in three dimensions). The LU implicit scheme was demonstrated to be efficient and robust for external flows in a broad flow regime and can be easily applied to internal flows and extended from two to three dimensions.

INTRODUCTION

The generation of a good grid is essential to obtaining by numerical simulation an accurate solution for the complex fluid flow phenomena in a turbine. A smooth and nearly orthogonal H-grid can be generated if the turbine blades are thin and have only a slight camber and sharp leading and trailing edges. But such geometry is rare for a turbine because of the high work factor desired from the turbine and the mechanical factors to be considered in designing the blades, which usually operate at high temperature and speed (ref. 1). Turbine blades are often designed to have substantial thickness and camber and rounded leading and trailing edges. Geometries are more complicated in the radial-inflow turbine than in the axial turbine. A typical radial-inflow turbine

*Summer faculty fellow.

rotor, for instance, turns the flow in 90° deflection in the meridional plane while simultaneously turning the flow in the blade-to-blade plane. Two representative turbine geometries are used to examine the grid generation for turbines: a radial-inflow turbine rotor (e.g., ref. 2) and an annular turbine stator (e.g., ref. 3).

For a typical turbine blade no single grid offers satisfactory grid properties in the entire rotor or stator passage. With the H-grid it is difficult to obtain a good boundary-layer resolution around the leading edge. If very fine meshes are used to resolve this, the number of grid points in the upstream region becomes excessive. Thus mesh points would be wasted. With the standard C-grid (or O-grid), for a typical turbine geometry, the grid becomes very skewed because the blades are highly cambered and the blade-to-blade grid lines curve sharply in the midpassage region (refs. 4 and 5).

A two-dimensional O/H patched grid used in a turbine cascade computation (ref. 6) shows the slope discontinuity at the O-H grid interface and has extremely large-aspect-ratio meshes near the leading edge. The numerical scheme used in that work is a cell-centered scheme based on the Beam and Warming approximate factorization (ref. 7). Although the flexibility of the scheme is indicated in two dimensions, its likely limitations in three dimensions suggest an alternative approach.

In this study two- and three-dimensional composite grids were generated in an attempt to improve the grid quality in terms of smoothness, resolution, and orthogonality. A numerical scheme that will run on this composite grid is discussed.

STANDARD GRIDS FOR TURBINE GEOMETRIES

A three-dimensional inviscid analysis using a H-grid was performed for the radial-inflow turbine rotor (ref. 8). The rotor used in the analysis is shown in figure 1. The rotor had 12 full blades thick enough to allow internal cooling passages and trailing-edge coolant ejection. The rotor had unswept radial blades at the inducer inlet and large blockages resulting from the thick trailing edges. In figure 2 the rotor surface is defined by using some of the grid lines on the rotor surface. Three-dimensional meshes in the radial turbine passage are shown in figure 3. As an illustration, only a selected number of grid lines on a selected number of grid surfaces are shown in the figure. A detailed H-grid for a blade-to-blade surface is shown in figure 4(a). The mesh on a meridional plane is shown in figure 5(a). Nonuniform grid spacing was used in all three directions. The quasi-orthogonal mesh lines were clustered near the leading and trailing edges, as illustrated in figures 4(a) and 5(a). In addition, this feature was also used to position the initial upstream grid at any desired location with a selected number of orthogonal grid lines and to position the final downstream grid where the experimental data were measured so that outputs from the inviscid calculation could be directly compared with experimental results. In the H-grid, cusps were required at the leading and trailing edges to get convergence of flow solution. Figure 4(a) shows the grid skewness for the leading edge; figure 4(b) shows the rapid velocity change near the leading edge. In spite of the difficult blade geometry (i.e., thick edges, large trailing blockage, turning of the passage in the meridional and blade-to-blade directions simultaneously, etc.), the three-dimensional inviscid analysis predicted the flow field reasonably well in a qualitative sense. But a large

entropy change occurred around the leading-edge region. As an example of results obtained from the three-dimensional inviscid analysis, figure 5(b) shows secondary velocity vectors on cross-channel surfaces.

A stator vane ring is shown in figure 6(a). The full annular ring consisted of 36 vanes. A sector of four vanes used to make laser anemometer measurements is shown. This vane ring was used for an annular cascade experiment reported in reference 3. The stator vane geometry is shown in figure 6(b). The vanes were untwisted, had a constant profile from hub to tip, and had a height of 38.10 mm and an axial chord of 38.23 mm. The vane aspect ratio and the solidity at the mean radius (based on axial chord) were 1.0 and 0.93, respectively. The stator hub-tip radius ratio was 0.85 and the tip diameter was 508 mm. The stacking axis of the vane was located at the center of the trailing-edge circle. To alleviate numerical errors associated with the H-grid skewness for the blunt leading edge, a standard C-grid was generated to examine any possible advantage over the H-grid for this turbine vane geometry (fig. 7(a)). The grid shows large skewing on the suction side of the blade passage (fig. 7(b)). Results of numerical simulations using this grid are likely to be affected by the grid skewing, as indicated in references 5 and 6.

COMPOSITE GRID

Two- and three-dimensional composite grids were generated for the turbine vanes of reference 3 (figs. 8(a) and (b), respectively). The blades were untwisted and stacked at the trailing edge (fig. 8(c)). Only a selected number of grid lines are shown for illustration. This composite grid consists of the C-grid (or O-grid) in the immediate vicinity of the blades and the H-grid in the upstream region and in the middle of the blade passage between the C-grids. The C-grid (or O-grid) portion can be generated by using either the elliptic method (ref. 9) or the algebraic method (ref. 10). At the C-grid and H-grid interface (or O-H interface) the slope continuity was preserved so that no special numerical approximations are needed for the derivatives at the interface. The C-grid (or O-grid) is orthogonal to the blade surface and provides a good boundary-layer resolution near the leading edge. This composite grid has better smoothness, resolution, and orthogonality than any type of single grid for a typical turbine blade with large camber and rounded leading and trailing edges.

For the two-dimensional grid in figure 8(a) the C-grid in the vicinity of the blade was generated by the elliptic grid generation code (ref. 11). Only a portion of the C-grid near the blade was retained for the composite grid. In the C-grid shown in figure 9, for instance, the portion between $\eta = 0$ and $\eta = \eta_C < \eta_{max}$ was retained, where $\eta = 0$ and $\eta = \eta_{max}$ are inner and outer boundaries, respectively, and choice of η_C is arbitrary and depends on the extent of the shear flow region. Then the H-grid was smoothly patched with the C-grids on the pressure and suction sides. At the C-H interface the slope continuity was preserved. The cubic spline and a stretching function were used to generate the H-grid in the midpassage and upstream regions. The three-dimensional grid in figure 8(b) was constructed algebraically from the two-dimensional composite grids of the hub and shroud surfaces.

NUMERICAL SCHEME

Semidiscrete Finite-Volume Scheme

The two-dimensional C-H composite grid has an unusual grid point that is connected to more than four neighboring nodes (fig. 10(a)). At this point the usual differencing techniques cannot be applied. If a standard finite-difference scheme were used to solve a flow problem on this composite grid, it would be difficult to treat this special point. A finite-volume scheme (ref. 12) to be used with this composite grid presents no problem and requires no special treatment because each interior cell of this composite grid has only four neighboring cells in two dimensions and six neighboring cells in three dimensions (fig. 10(b)). The finite-volume scheme is described briefly here.

The Euler equations in integral form can be written as

$$\frac{\partial}{\partial t} \iiint_{\Omega} w \, d\Omega + \iint_{\partial\Omega} \underline{F} \cdot d\underline{S} = 0 \tag{1}$$

for a fixed region Ω with boundary $\partial\Omega$. Here w represents the conserved quantity, $\underline{F}$ is the corresponding flux term, and t is time.

A convenient way to ensure a steady-state solution independent of the time step is to separate the space and time discretization procedures. In the semidiscrete finite-volume scheme one begins by applying a semidiscretization in which only the spatial derivatives are approximated. To derive a semidiscrete model that can be used to treat complex geometric domains, the computational domain is divided into quadrilateral cells. Assuming that the dependent variables are known at the center of each cell, a system of ordinary differential equations is obtained by applying equation (1) separately to each cell. These have the form

$$\frac{d}{dt} (S_{ij} w_{ij}) + Q_{ij} = 0 \tag{2}$$

where S_{ij} is the cell area and Q_{ij} is the net flux out of the cell. This can be evaluated as

$$\sum_{k=1}^{4} (\Delta y_k \, f_k - \Delta x_k \, g_k) \tag{3}$$

where f_k and g_k denote values of the flux vectors $\underline{f}$ and $\underline{g}$ on the k^{th} edge, Δx_k and Δy_k are the increments of x and y along the edge with appropriate signs, and the sum is over the four sides of the cell. The flux vectors are evaluated by averaging the values in the cells on either side of the edge:

$$f_1 = \frac{1}{2} (f_{i+1,j} + f_{i,j})$$

for example. The scheme constructed in this manner reduces to a central difference scheme on a Cartesian grid and is second-order accurate in space provided that the mesh is smooth enough. It also has the property that uniform flow is an exact solution of the difference equations.

LU Implicit Scheme

The composite grid is generated to be used for both inviscid and viscous flow calculations. For viscous calculations the C- or O-meshes must be very fine to resolve the boundary layer. And it is likely that the time step imposed by an explicit stability bound will be much less than that imposed by the accuracy bound of an implicit scheme. Since an obvious way to accelerate convergence to a steady state is to increase the size of the time step, an implicit scheme is expected to have a faster convergence. Although the alternating direction implicit (ADI) scheme has been valuable in two-dimensional problems, its inherent limitations in three dimensions suggest an alternative approach. A LU implicit scheme (ref. 13) was demonstrated to be efficient and robust for external flows in a broad flow regime and can be readily extended from two to three dimensions. This scheme, briefly discussed here, will be used for the numerical simulation of turbine flows.

The conservation law form of the Euler equations in Cartesian coordinates for two-dimensional flow is

$$\frac{\partial \underline{W}}{\partial t} + \frac{\partial \underline{F}}{\partial x} + \frac{\partial \underline{G}}{\partial y} = 0 \tag{4}$$

where $\underline{W}$ is the vector of dependent variables and $\underline{F}$ and $\underline{G}$ are convective flux vectors:

$$\begin{aligned} \underline{W} &= (\rho, \rho u, \rho v, \rho E)^T \\ \underline{F} &= [\rho u, \rho u^2 + p, \rho vu, u(\rho E + p)]^T \\ \underline{G} &= [\rho v, \rho uv, \rho v^2 + p, v(\rho E + p)]^T \end{aligned} \tag{5}$$

where ρ, u, v, E, and p are density, velocity components, total energy, and pressure. The pressure is obtained from the equation of state

$$p = \rho(\gamma - 1)\left[E - \frac{1}{2}(u^2 + v^2)\right] \tag{6}$$

where γ is the ratio of heat capacity at constant pressure to heat capacity at constant volume. These equations are to be solved for a steady-state $\partial \underline{W}/\partial t = 0$, where t denotes time.

Let the Jacobian matrices be

$$A = \frac{\partial \underline{F}}{\partial \underline{W}} \quad , \quad B = \frac{\partial \underline{G}}{\partial \underline{W}}$$

and let the correction be

$$\delta \underline{W} = \underline{W}^{n+1} - \underline{W}^n$$

where n denotes the time level.

The linearized implicit scheme for a system of nonlinear hyperbolic equations such as the Euler equations can be formulated as

$$\left[I + \beta\,\Delta t\,(D_x A + D_y B)\right]\,\delta\underline{W} + \Delta t\,\underline{R} = 0 \qquad (7)$$

where I is the identity matrix and $\underline{R}$ is the residual

$$\underline{R} = D_x\underline{F}(\underline{W}^n) + D_y\underline{G}(\underline{W}^n)$$

Here D_x and D_y are central difference operators that approximate $\partial/\partial x$ and $\partial/\partial y$.

If $\beta = 1/2$ the scheme remains second-order accurate in time; for other values of β the time accuracy drops to first order. The unfactored implicit scheme (eq. (7)) produces a large block-banded matrix, which is very costly to invert and requires huge storage. An unconditionally stable implicit scheme that has error terms at most of order $(\Delta t)^2$ in any number of space dimensions can be derived by LU factorization

$$\left[I + \beta\,\Delta t\,(D_x^- A^+ + D_y^- B^+)\right]\left[I + \beta\,\Delta t\,(D_x^+ A^- + D_y^+ B^-)\right]\,\delta\underline{W} + \Delta t\,R = 0 \qquad (8)$$

where $D_{\bar{x}}$ and $D_{\bar{y}}$ are backward difference operators and D_x^+ and D_y^+ are forward difference operators. The reason for splitting is to ensure the diagonal dominance of lower and upper factors as well as to make use of the built-in implicit dissipation.

Here A^+, A^-, B^+, and B^- are constructed so that the eigenvalues of "+" matrices are nonnegative and those of "-" matrices are nonpositive.

$$A^+ = \frac{1}{2}(A + r_A I), \qquad A^- = \frac{1}{2}(A - r_A I)$$

$$B^+ = \frac{1}{2}(B + r_B I), \qquad B^- = \frac{1}{2}(B - r_B I)$$

where

$$r_A \geq \max(|\lambda_A|), \qquad r_B \geq \max(|\lambda_B|)$$

Here λ_A and λ_B represent eigenvalues of Jacobian matrices. Equation (8) can be inverted in two steps. The LU implicit scheme needs the inversion of sparse triangular matrices, which can be done efficiently without using large storage. This scheme has only two factors in three dimensions.

CONCLUDING REMARKS

Two- and three-dimensional composite grids were generated in an attempt to improve grid quality in terms of smoothness, resolution, and orthogonality for an annular turbine cascade. This composite grid, which has a C-type (or O-type) grid in the immediate vicinity of the turbine blade, provides a good boundary-layer resolution around the leading-edge region for viscous calculation, has orthogonality at the blade surface and slope continuity at the C-H (or O-H) interface, and controls mesh distribution in the upstream region without using excessive grid points. This composite grid eliminates the undesirable qualities of a single grid when generated for a typical turbine geometry.

A finite-volume lower-upper (LU) implicit scheme can be used in solving for the turbine flows on the composite grid. This grid has a special grid node

that is connected to more than four neighboring nodes in two dimensions and to more than six nodes in three dimensions. But the finite-volume approach poses no problem at the special point because each interior cell has only four neighboring cells in two dimensions and only six cells in three dimensions. The LU implicit scheme was proved to be efficient in a broad flow regime and is expected to yield accurate solutions on the improved composite grid.

REFERENCES

1. Glassman, A.J.: Turbine Design and Application, Vol. 2, NASA SP-290-vol-2, 1973.

2. McLallin, K.L.; and Haas, J.E.: Experimental Performance and Analysis of 15.04-cm-Tip-Diameter, Radial-Inflow Turbine with Work Factor of 1.126 and Thick Blading. NASA TP-1730, 1980.

3. Goldman, L.J.; and Seasholtz, R.G.: Laser Anemometer Measurements in an Annular Cascade of Core Turbine Vanes and Comparison with Theory. NASA TP-2018, 1982.

4. Steger, J.L.: On Application of Body Conforming Curvilinear Grids for Finite Difference Solution of External Flow. Numerical Grid Generation, J.F. Thompson, ed., North-Holland, 1982, pp. 295-316.

5. Davis, R.L.; Ni, R.H.; and Carter, J.E.: Cascade Viscous Flow Analysis Using the Navier-Stokes Equations. AIAA Paper 86-0033, Jan. 1986.

6. Norton, R.J.G.; Thompkins, W.T., Jr.; and Haimes, R.: Implicit Finite-Difference Schemes with Non-Simply-Connected Grids - A Novel Approach, AIAA Paper 84-0003, Jan. 1984.

7. Beam, R.M.; and Warming, R.F.: An Implicit Factored Scheme for the Compressible Navier-Stokes Equations. AIAA J., vol. 16, no. 4, Apr. 1978, pp. 393-402.

8. Choo, Y.K.; and Civinskas, K.C.: Three-Dimensional Inviscid Analysis of Radial-Turbine Flow and a Limited Comparison with Experimental Data. Three-Dimensional Flow Phenomena in Fluid Machinery, A. Hamed, H.J. Herring, and L.A. Povinelli, eds., ASME FED. Vol. 32, ASME, 1985, pp. 181-190.

9. Thompson, J.F.; Thames, F.C.; and Mastin, C.W.: Automatic Numerical Generation of Body-Fitted Curvilinear Coordinate System for Field Containing Any Number of Arbitrary Two-Dimensional Bodies. J. Comput. Phys., vol. 15, no. 3, July 1974, pp. 299-319.

10. Eiseman, P.R.; and Smith, R.E.: Mesh Generation Using Algebraic Techniques. Numerical Grid Generation Techniques, NASA CP-2166, 1980, pp. 73-120.

11. Sorenson, R.L.: A Computer Program to Generate Two-Dimensional Grids About Airfoils and Other Shapes by the Use of Poisson's Equation. NASA TM-81198, 1980.

12. Jameson, A.; and Yoon, S.: Multigrid Solution of the Euler Equations Using Implicit Schemes. AIAA Paper 85-0293, Jan. 1985.

13. Jameson, A.; and Yoon, S.: LU Implicit Schemes with Multiple Grids for the Euler Equations. AIAA Paper 86-0105, Jan. 1986.

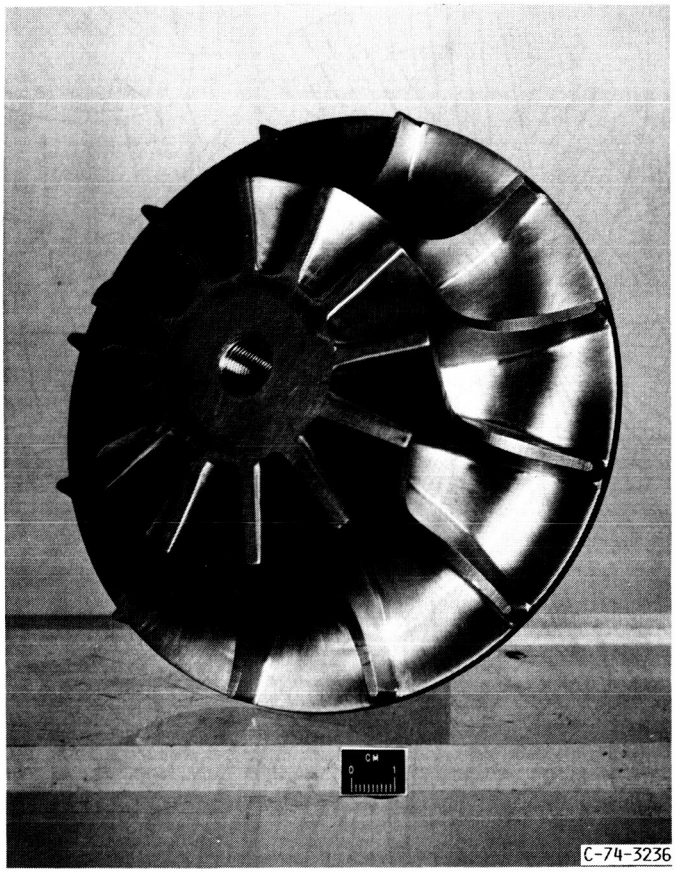

Figure 1. - Radial inflow turbine rotor.

ORIGINAL PAGE

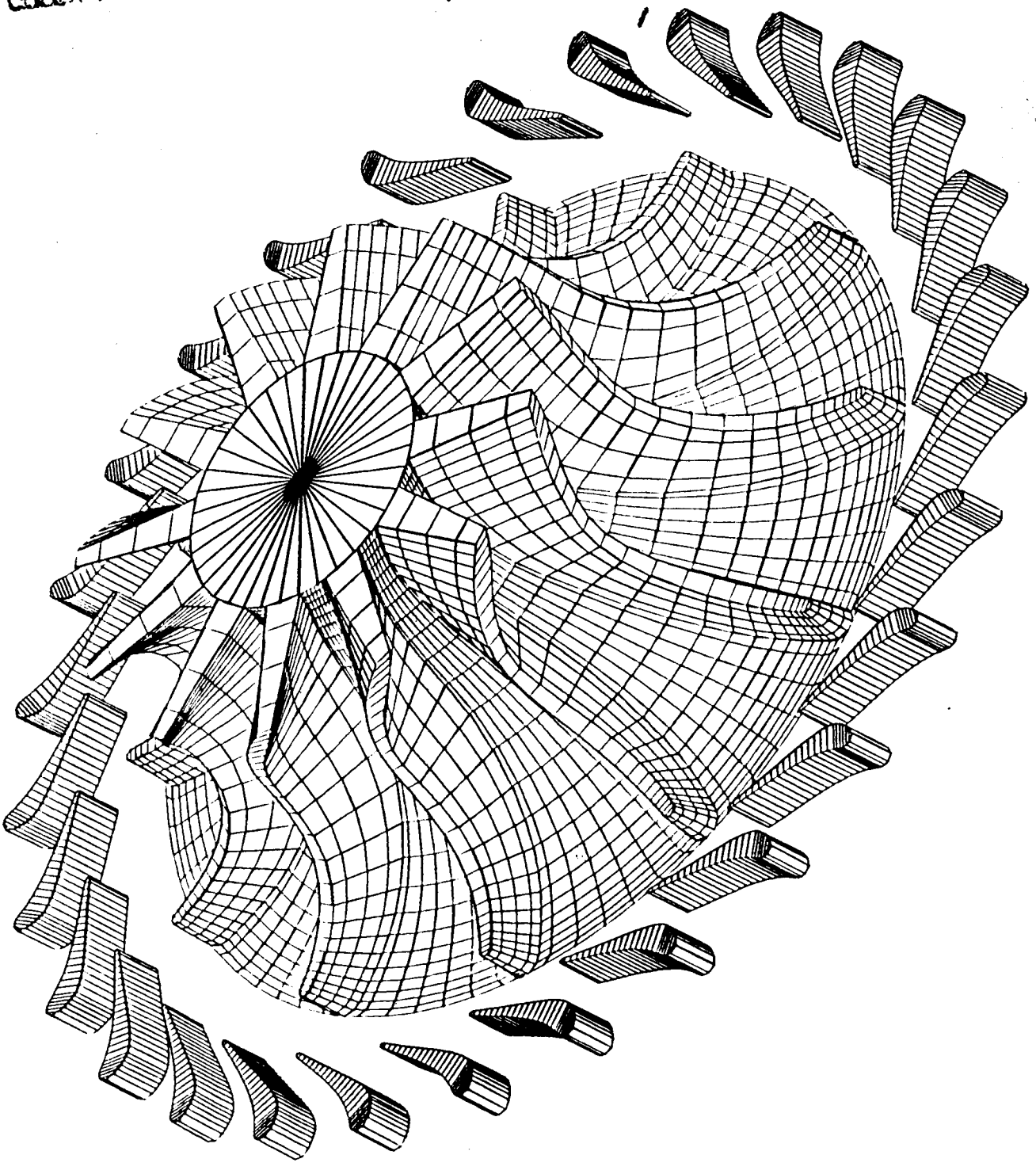

Figure 2. - Surface definition of radial-inflow turbine.

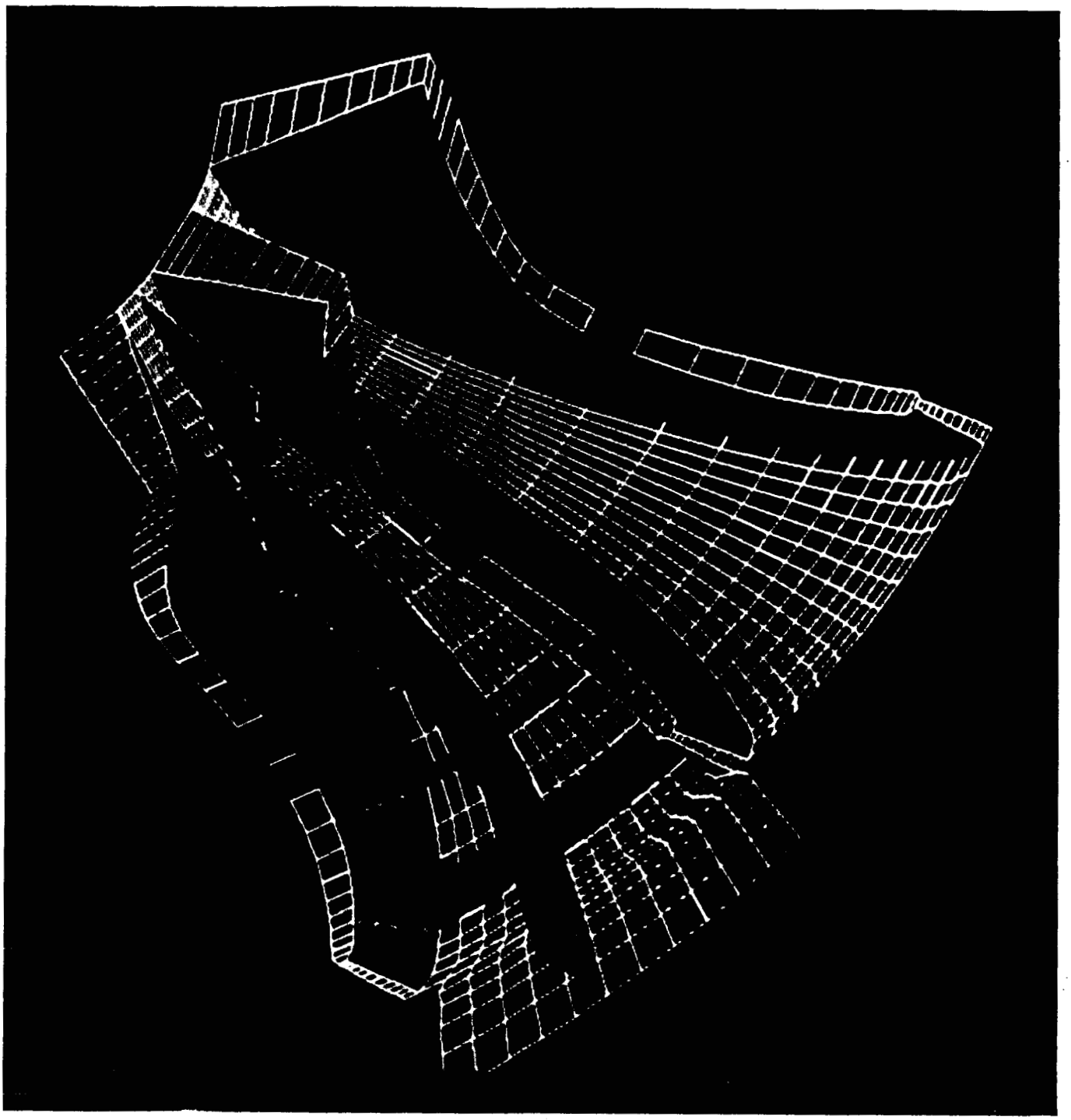

Figure 3. - Three-dimensional meshes in radial turbine passage.

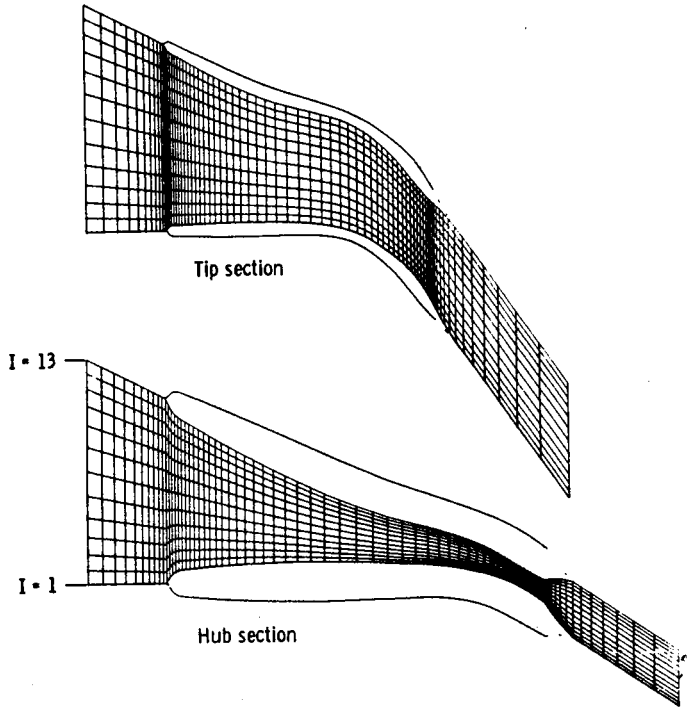

(a) Grids on blade-to-blade surface.

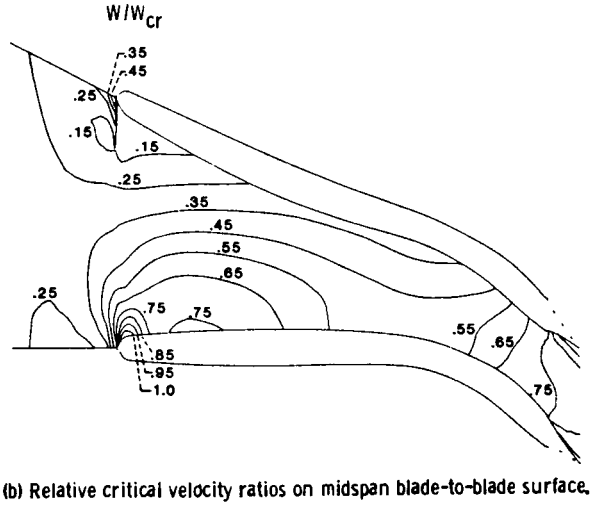

(b) Relative critical velocity ratios on midspan blade-to-blade surface.

Figure 4. - Velocity contours on blade-to-blade surface (from three-dimensional inviscid computation).

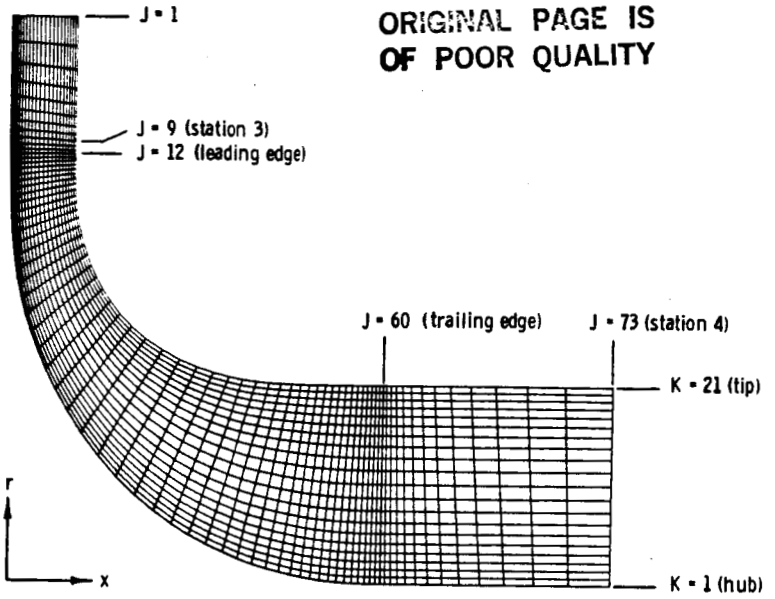

(a) Grid in meridional plane.

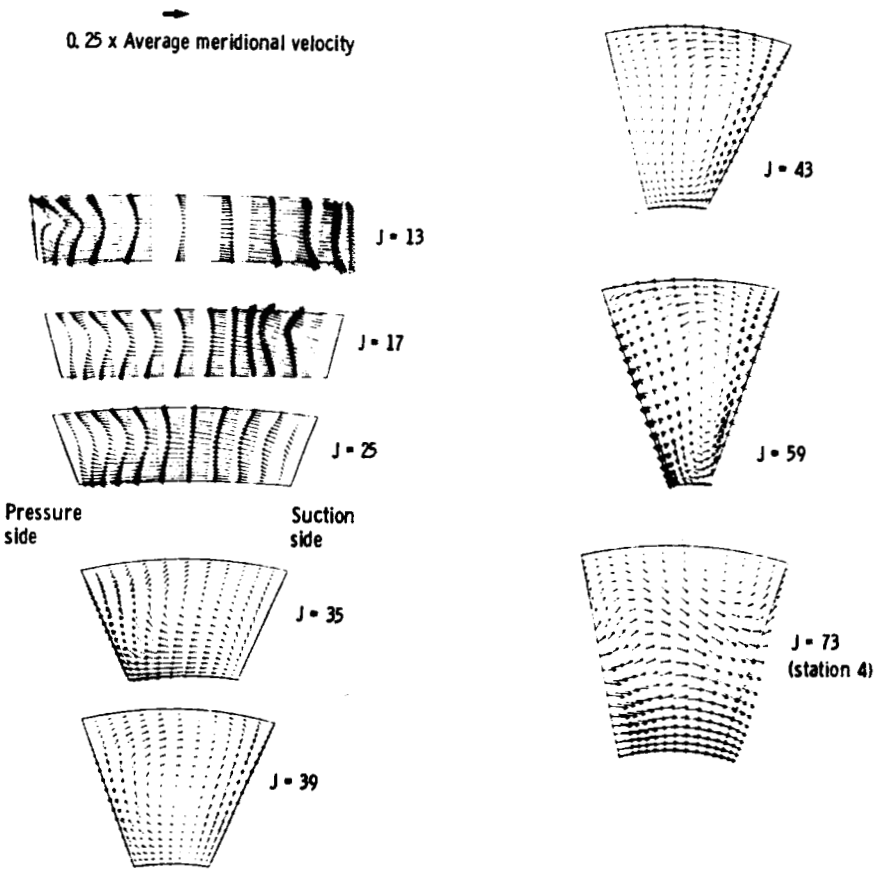

(b) Secondary velocity vectors on cross-channel surfaces.

Figure 5. - Evolution of passage vortex (from three-dimensional inviscid computation).

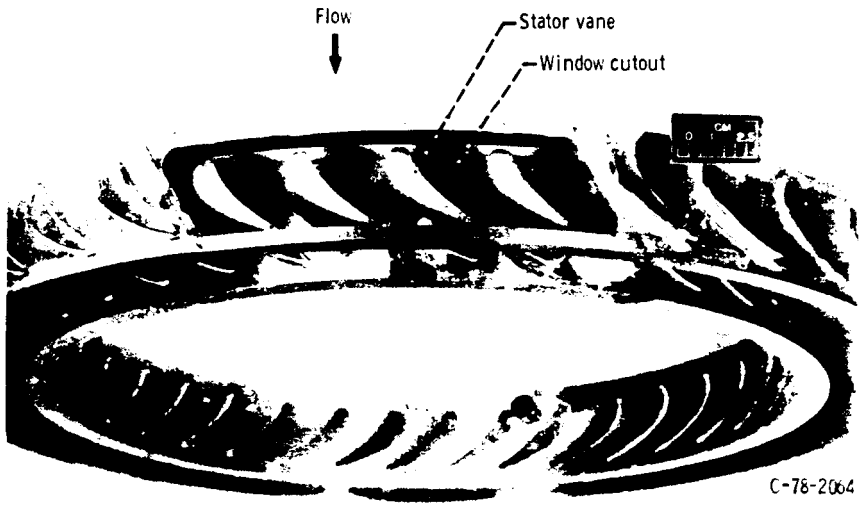

(a) Ring showing cutout for laser window.

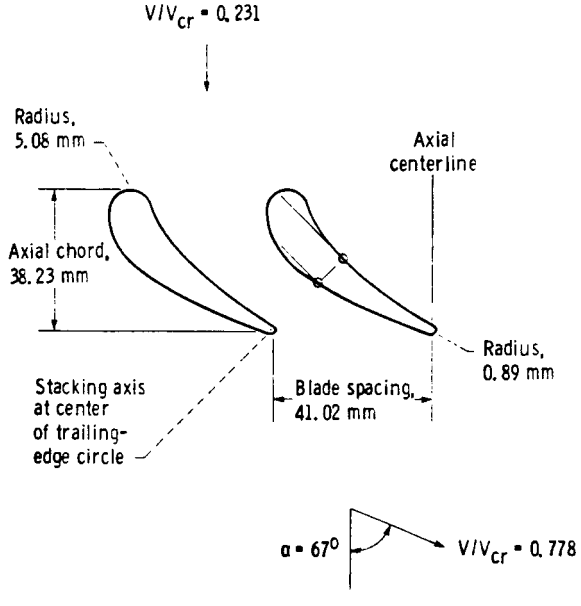

(b) Geometry at mean section. (V/V_{cr} = critical velocity ratio.)

Figure 6. - Core turbine stator vane.

ORIGINAL PAGE
COLOR PHOTOGRAPH

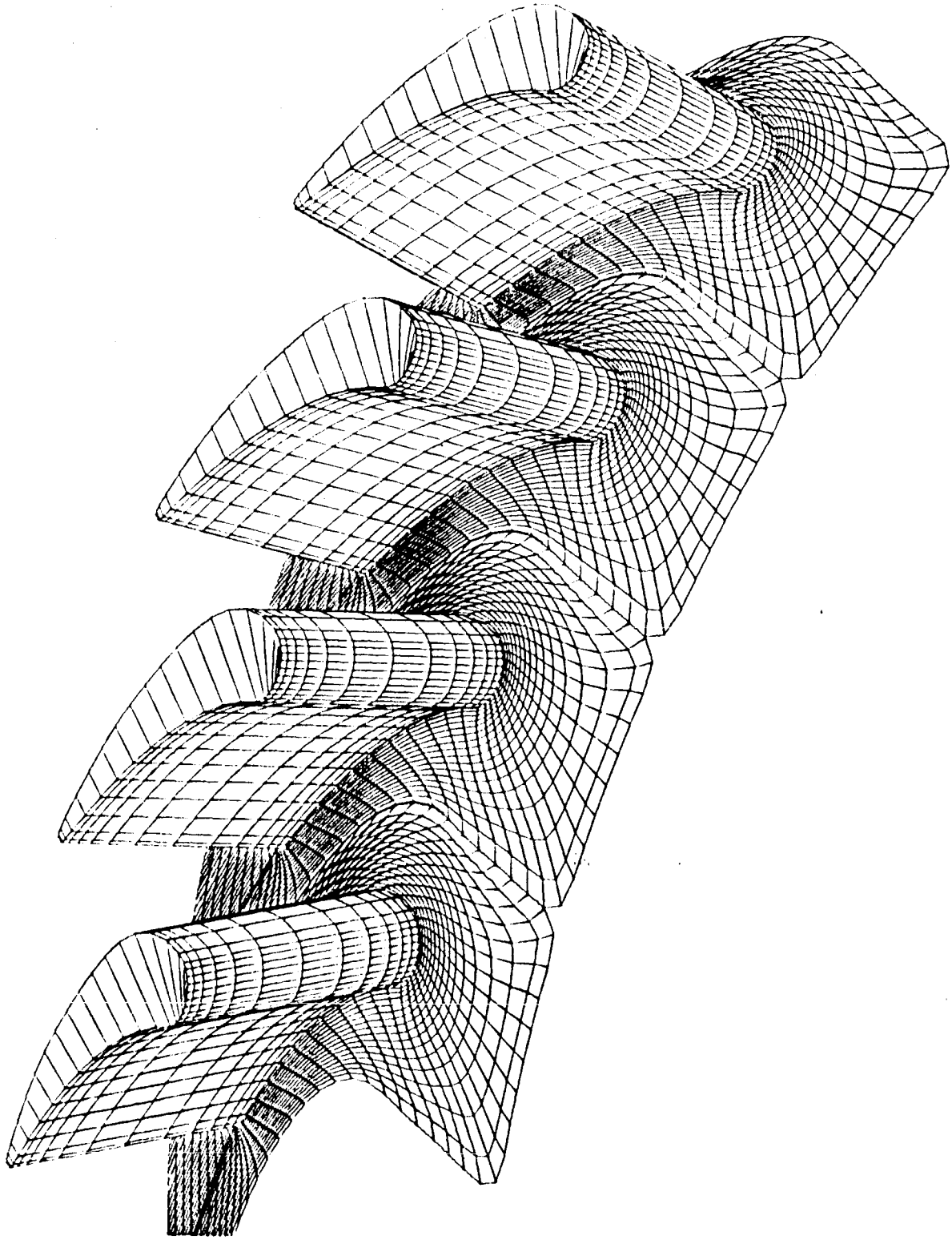

(a) Three dimensions.

Figure 7. - Standard C-grid for turbine stator vanes of annular cascade.

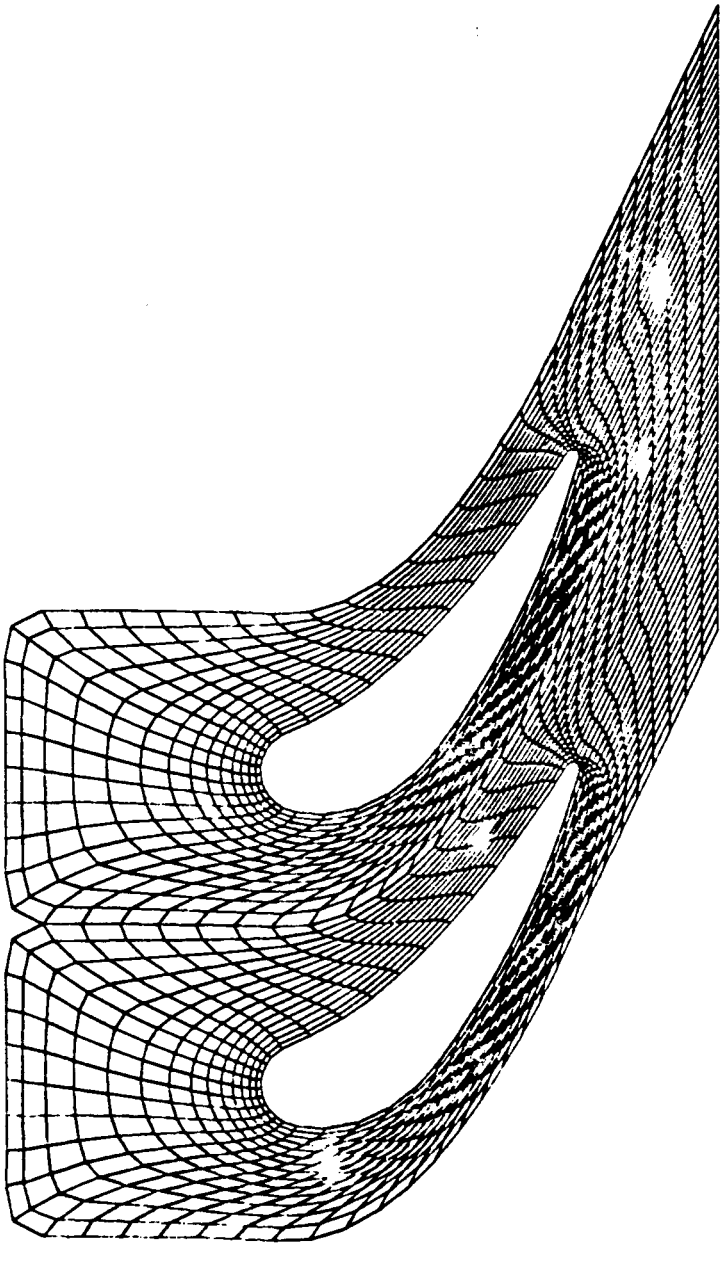

(b) Two dimensions.

Figure 7. - Concluded.

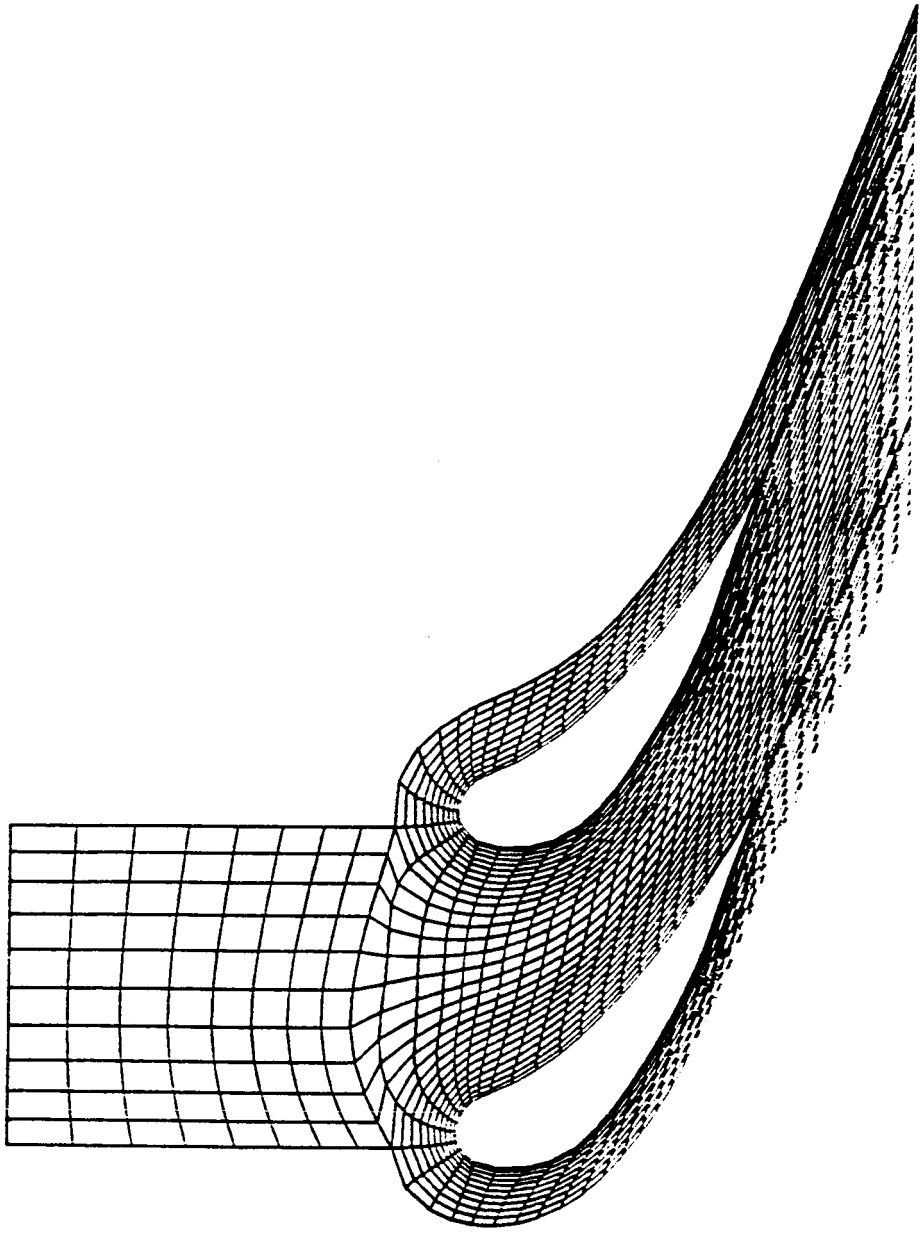

(a) Two dimensions.

Figure 8. - Composite grid for turbine stator vanes of annular cascade.

ORIGINAL PAGE
COLOR PHOTOGRAPH

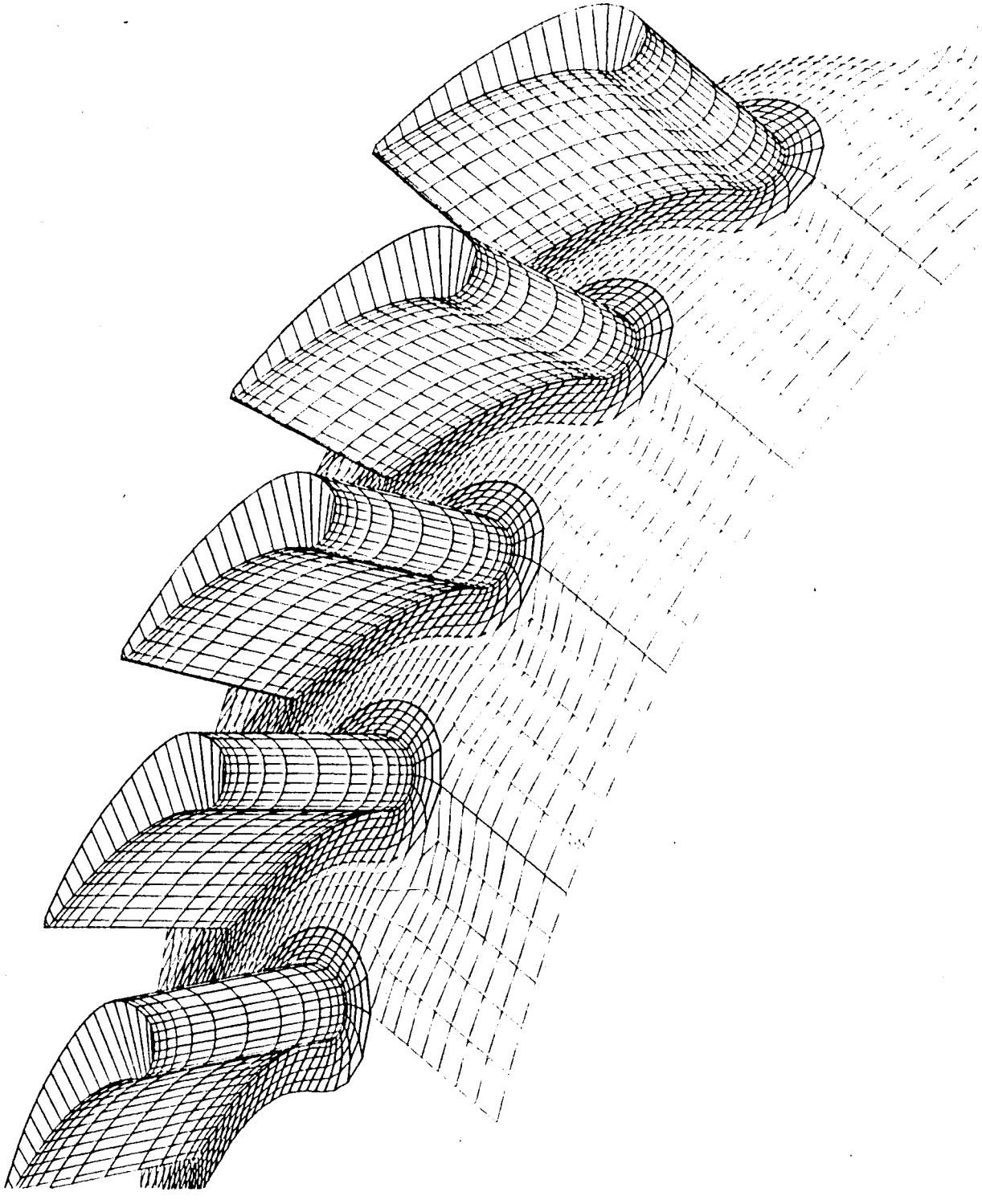

(b) Three dimensions.

Figure 8. - Continued.

ORIGINAL PAGE
COLOR PHOTOGRAPH

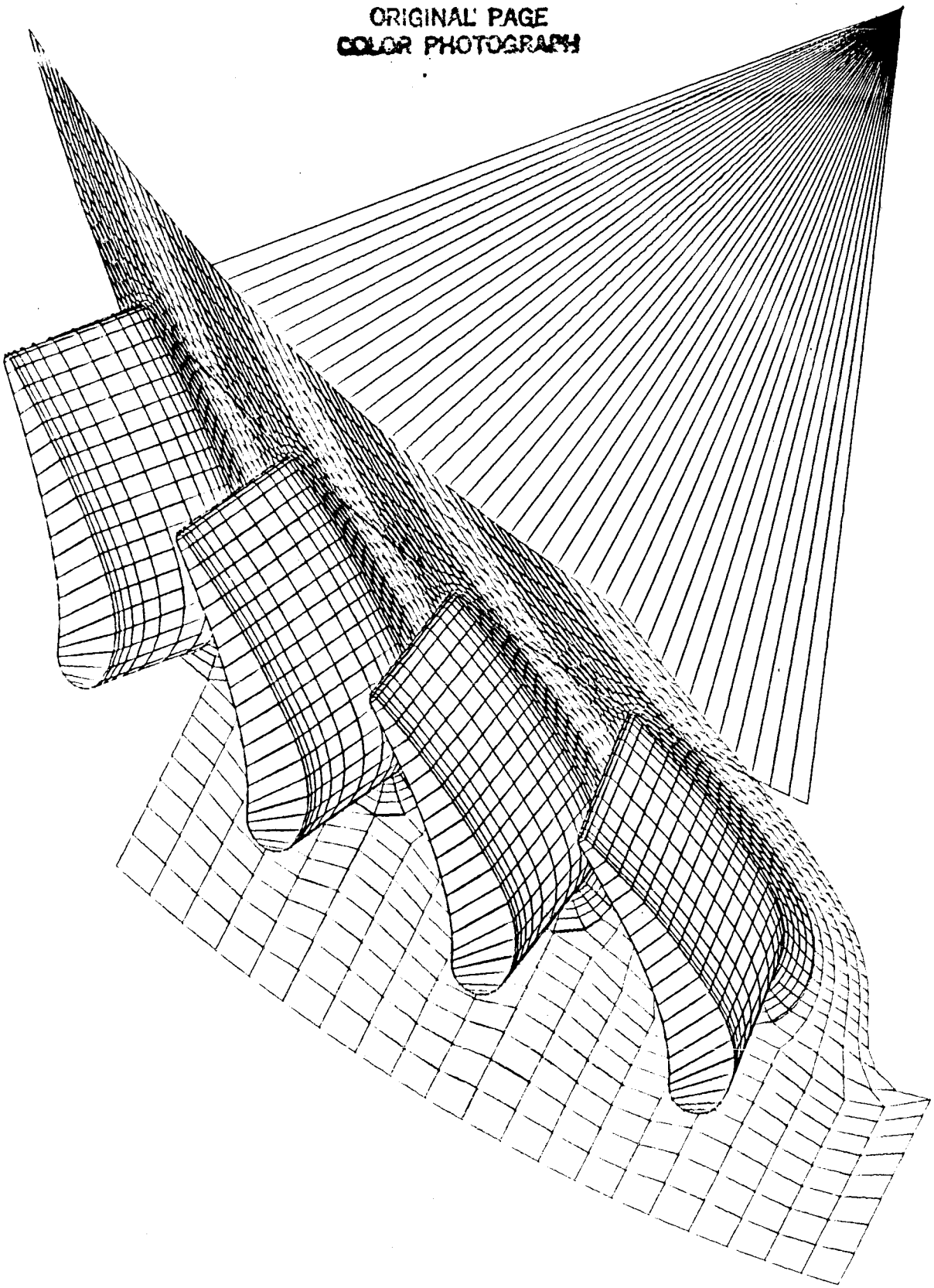

(c) Stacked at trailing edges.

Figure 8. - Concluded.

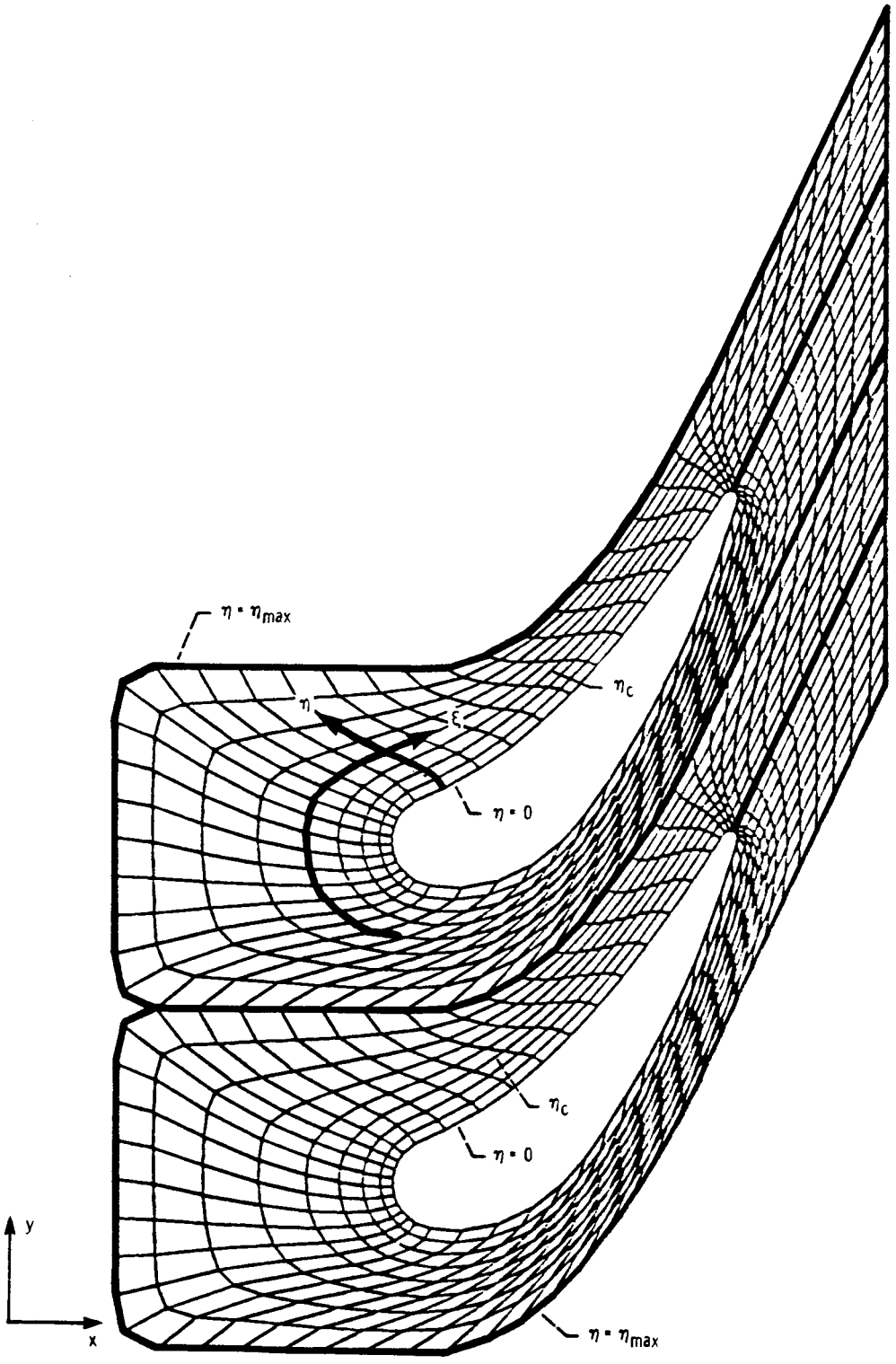

Figure 9. - Standard two-dimensional C-grid for turbine stator vanes of annular cascade, with ξ and η coordinates shown.

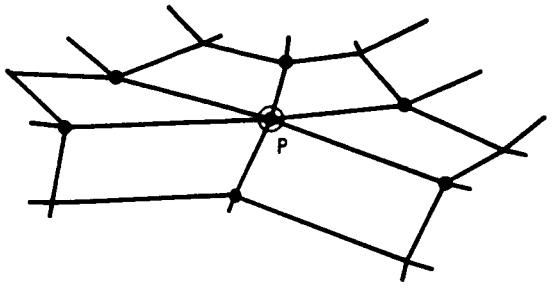

(a) Grid nodes to be used in finite-difference scheme.

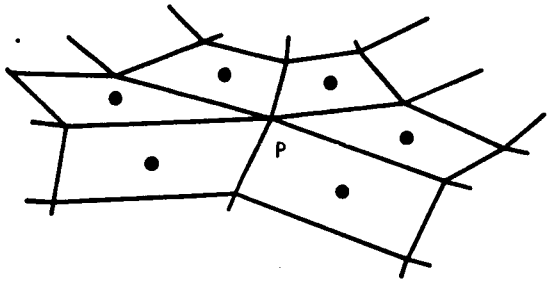

(b) Cell centers to be used in finite-volume scheme.

Figure 10. - Special point of composite grid.

1. Report No.	2. Government Accession No.	3. Recipient's Catalog No.
NASA TM-88890 USAAVSCOM-TR-86-C-38		

4. Title and Subtitle	5. Report Date
Generation of a Composite Grid for Turbine Flows and Consideration of a Numerical Scheme	November 1986
	6. Performing Organization Code

7. Author(s)	8. Performing Organization Report No.
Y. Choo, S. Yoon, and C. Reno	E-3301
	10. Work Unit No.

9. Performing Organization Name and Address	11. Contract or Grant No.
NASA Lewis Research Center and Propulsion Directorate, U.S. Army Aviation Research and Technology Activity - AVSCOM, Cleveland, Ohio 44135	
	13. Type of Report and Period Covered
12. Sponsoring Agency Name and Address	Technical Memorandum
National Aeronautics and Space Administration Washington, D.C. 20546 and U.S. Army Aviation Systems Command, St. Louis, Mo 63120	14. Sponsoring Agency Code

15. Supplementary Notes

Y. Choo, Lewis Research Center; S. Yoon, Sverdrup Technology, Inc., Lewis Research Center, Cleveland, Ohio 44135; C. Reno, Summer Faculty Fellow, Propulsion Directorate, U.S. Army Aviation Research and Technology Activity - AVSCOM.

16. Abstract

A composite grid was generated for flows in turbines. It consisted of the C-grid (or O-grid) in the immediate vicinity of the blade and the H-grid in the middle of the blade passage between the C-grids and in the upstream region. This new composite grid provides better smoothness, resolution, and orthogonality than any single grid for a typical turbine blade with a large camber and rounded leading and trailing edges. The C-H (or O-H) composite grid has an unusual grid point that is connected to more than four neighboring nodes in two dimensions (more than six neighboring nodes in three dimensions). A finite-volume lower-upper (LU) implicit scheme to be used on this grid poses no problem and requires no special treatment because each interior cell of this composite grid has only four neighboring cells in two dimensions (six cells in three dimensions). The LU implicit scheme was demonstrated to be efficient and robust for external flows in a broad flow regime and can be easily applied to internal flows and extended from two to three dimensions.

17. Key Words (Suggested by Author(s))	18. Distribution Statement
Grid generation Numerical scheme Turbomachinery	Unclassified - unlimited STAR Category 02

19. Security Classif. (of this report)	20. Security Classif. (of this page)	21. No. of pages	22. Price*
Unclassified	Unclassified		

*For sale by the National Technical Information Service, Springfield, Virginia 22161